

In-beam γ -ray spectroscopy of the $N = Z + 1$ nucleus ^{63}Ga

D. P. Balamuth, U. J. Hüttmeier, T. Chapuran,* D. G. Popescu, and J. W. Arrison

Department of Physics, University of Pennsylvania, Philadelphia, Pennsylvania 19104

(Received 19 December 1990)

A total of ten previously observed γ rays have been assigned to the $N = Z + 1$ nucleus ^{63}Ga ; these provide the first information on excited states reported in this neutron-deficient system. ^{63}Ga has been populated using the $^{40}\text{Ca}(^{28}\text{Si}, \alpha p)$, $^{40}\text{Ca}(^{32}\text{S}, 2\alpha p)$, and $^{40}\text{Ca}(^{29}\text{Si}, \alpha pn)$ reactions at beam energies of 80–100 MeV. Particle- γ coincidence techniques provide a definitive identification of γ transitions in ^{63}Ga . An yrast-level scheme is proposed on the basis of charged-particle- γ , charged-particle- γ - γ , and neutron- γ - γ coincidences. Spin and parity assignments are based on neutron-gated γ -ray angular distributions, directional correlation with oriented nuclei ratios and systematics. Nine new energy levels are identified in addition to the previously known ground state, with the highest level at an excitation energy of 7.7 MeV. The results are interpreted in terms of the relevant single-particle orbitals and the systematics of the neighboring nuclei. In addition, a new determination has been made of the $E2/M1$ mixing ratio for the $(\frac{5}{2}^-)_1 \rightarrow (\frac{3}{2}^-)_1$ transition in ^{65}Ga , resolving a disagreement between two previous measurements.

I. INTRODUCTION

Nuclei far from the valley of β stability have proven to be an excellent testing ground for nuclear models involving single-particle and collective degrees of freedom. Recently developed experimental techniques, such as 4π charged-particle detectors operated in coincidence with high-resolution Ge detectors, have permitted the application of in-beam γ -ray spectroscopy to quite neutron-deficient systems. As an example in the mass $60 < A < 70$ region, an yrast level scheme for the $N = Z + 1$ system ^{65}Ge ($Z = 32$) was recently studied; in addition, several γ rays in the $N = Z$ nucleus ^{64}Ge were identified using similar methods combined with the simultaneous detection of evaporation neutrons (Ref. 1).

One of the most powerful tools for understanding structural changes as a function of N and Z in this mass region has been the examination of the interaction between an odd particle in a unique parity orbital, usually a Nilsson orbital originating in the $g_{9/2}$ shell-model state, and the core. For example, in ^{65}Ge it was found that a $\frac{15}{2}^-$ state, conjectured to be formed by weakly coupling a $g_{9/2}$ neutron to a 3^- vibration of the ^{64}Ge core, was strongly lowered in energy compared to the systematics of neighboring nuclei. This is of considerable interest in view of theoretical predictions² of softness towards octupole deformation in the vicinity of ^{64}Ge . The odd particle can also be used to probe the nature of quadrupole collectivity in the core as a function of N and Z . For example, in the light odd- A Br isotopes ($Z = 35$), including the recently studied $N = Z + 1$ system ^{71}Br , the odd proton appears to stabilize prolate deformation in the core,^{3,4,5} whereas in the lightest odd- N Se isotopes ($Z = 34$) the best currently available experimental evidence favors oblate deformation of the core in the band built on the

$vg_{9/2}$ state.^{6,7}

Negative-parity states in the odd- A Ga isotopes ($Z = 31$) are mainly formed from couplings of the odd proton in fp -shell orbits to the neighboring even-even core. In many cases two low-lying $\frac{5}{2}^-$ states are known: in a very simplified picture these can be thought of as an $f_{5/2}$ proton coupled to the ground state of the core and an fp -shell proton coupled to the lowest 2^+ excited state of the core. The $E2$ component of the $(\frac{5}{2}^-)_j \rightarrow (\frac{3}{2}^-)_1$ transition in this picture is single-particle-like for the first state and has the same collectivity as the $2_1^+ \rightarrow 0_1^+$ transition in the core for the second one. The pattern in the well-known Ga isotopes ($A = 67, 69, 71$) is that the lowest $\frac{5}{2}^-$ state is single-particle-like, while the second $\frac{5}{2}^-$ state has a collective $E2$ transition to the lowest $\frac{3}{2}^-$ state of strength similar to that observed in the neighboring Zn cores.^{8,9,10} The data suggest very little mixing between these two states. A possible break in this pattern for the lightest odd- A Ga nucleus studied to date, ^{65}Ga , is suggested by the work of Kawakami *et al.*,¹¹ who measured the $E2/M1$ mixing ratio for the $(\frac{5}{2}^-)_1 \rightarrow (\frac{3}{2}^-)_1$ transition as $\delta = +0.7 \pm 0.3$, where we have changed the phase convention to that of Rose and Brink.¹² Taken with the existing limit¹³ on the lifetime of the $(\frac{5}{2}^-)_1$ $E_x = 191$ keV state, $T_{1/2} < 0.7$ ns, this would imply a strongly collective $E2$. An $E2/M1$ mixing ratio $\delta = 0.7 \pm 0.3$ and the lifetime limit corresponds to a lower limit on the $B(E2)$ of 28 W.u. (where W.u. represents Weisskopf unit), although it should be noted that the experimental error on the mixing ratio is sufficiently large that one must exercise caution before drawing firm conclusions. In addition, an earlier measurement of the same $E2/M1$ mixing ratio¹⁴ was consistent with a nearly pure $M1$ transition, in disagreement with Ref. 11. The possibility of a

discontinuous change in the collective properties of the odd Ga isotopes enhances the interest in the present study of the lightest known odd- A Ga isotope, $N = Z + 1$ ^{63}Ga , which in a more general way has been pursued to complement our previous studies (Ref. 1) on the structure of neutron-deficient nuclei in this mass region. Prior to this study information on the structure of ^{63}Ga was limited to a tentative spin and parity assignment of the ground state based on its nuclear beta decay.¹⁵ No excited states have been reported in the literature. In the course of this work we also reinvestigated some aspects of the low-lying levels of ^{65}Ga . New information was obtained which bears directly on the possibility suggested by the work of Ref. 11 of a strong $E2$ transition connecting the lowest negative parity states.

The paper is organized as follows. The experiments performed in order to provide a definitive identification of γ transitions in ^{63}Ga are described in the next section. We then proceed with the data analysis and results followed by a discussion of the level scheme deduced from these measurements. In the final section the decay scheme is compared to the systematics of neighboring nuclei and the structure of the yrast states is discussed in the framework of the weak-coupling model. Some of the results of the present work have been reported previously.¹⁶

II. EXPERIMENTAL PROCEDURE

Nuclei with $N \approx Z$ in the mass-64 region are difficult to produce with cross sections exceeding 10 mb, or about 1–2 % of the total fusion cross section. Accordingly, the identification of in-beam γ transitions requires the use of an experimental filter to separate the transitions of interest from the much more intense background from more prolific fusion-evaporation channels. The strategy employed in the present study has been to utilize coincidences between γ rays and light charged particles (protons and α particles) to identify transitions in ^{63}Ga . The identification has been checked using cross bombardment with different projectiles and verifying that the pattern of particle- γ coincidences observed is consistent with the reaction channel assumed. Excitation curves have been measured in selected cases as an aid to the identification process.

In cases where the nucleus of interest is produced using a reaction in which one or more neutrons are evaporated, neutron- γ coincidence measurements are also quite useful in the study of neutron-deficient nuclei in this region. Such a requirement eliminates the background from the (dominant) channels in which only charged particles are evaporated, thereby enhancing the peak-to-background ratio for the channel of interest. We have employed this technique in the present study to measure γ -ray angular distributions for candidate lines both in ^{63}Ga and in a n - γ - γ triple-coincidence experiment designed to construct a level scheme for ^{63}Ga . Some γ - γ coincidence data were also obtained in coincidence with charged particles (see below). All of the measurements described in this paper utilized beams of ^{28}Si , ^{29}Si , and ^{32}S accelerated with the University of Pennsylvania tandem Van de Graaff accelerator. In the following subsections we de-

scribe the experimental setup(s) for the measurements performed.

A. Charged-particle- γ coincidence measurements

All of the charged-particle- γ coincidences performed in this work utilized the University of Pennsylvania 4π phoswich array.¹⁷ The complete detector consists of 24 phoswich telescopes which cover approximately 90% of the full sphere. As noted in Ref. 17, the device was assembled in stages, and some of the work described in this paper utilized earlier versions of the detector in which $\frac{2}{3}$ (phase I) or $\frac{1}{3}$ (phase II) of the total solid angle was covered by veto detectors which recorded charged particles but gave no identification information. Such an arrangement preserves full 4π detection, essential to reject background from the much more prolific channels with higher charged-particle multiplicity, but has a lower detection efficiency than the completed detector.

The first identification of ^{63}Ga was performed using the data from our previous¹ experimental investigation of ^{65}Ge . In that experiment a 90-MeV beam of ^{28}Si was used to bombard a target consisting of $350 \mu\text{g}/\text{cm}^2$ of ^{40}Ca evaporated onto a $30\text{-mg}/\text{cm}^2$ gold backing. The backing served to stop the beam and the recoils and to shield the particle telescopes at forward angles from elastically scattered particles. The telescopes at backward angles were shielded from the elastically scattered beam using Ta absorbers. This first experiment utilized phase I of the 4π array. Five phoswich telescopes covering approximately $\frac{1}{3}$ of 4π were operated in coincidence with two unsuppressed 25% Ge detectors; the latter were placed at angles of 90° and 135° with respect to the incident beam at a distance of 9 cm from the target. The veto detectors covered the remaining fraction of 4π and were used to eliminate events in which charged particles were emitted in directions not covered by phoswiches (see Ref. 17).

Events involving one or more charged particles detected in coincidence with two γ rays were written in event mode to mass storage media for subsequent off-line analysis. This first phase-I experiment utilized 1600 bpi magnetic tape as the storage medium. Subsequent experiments utilized WORM (write-once-read-many) optical disks with a capacity of 1.6 Gbyte per side. Both on-line and off-line data analysis was performed with an array of microprocessors operating in parallel in the input data stream. Each processor incremented a common set of histograms using the VMEbus standard. A more complete description of the multiple processor system has recently been given elsewhere.¹⁸

An energy calibration for each of the 5 phoswich detectors was obtained using published values of the amount of scintillation light produced by protons and α particles.¹⁹ These calibrations are quite nonlinear at low energies, and are different for protons and α particles. A correct relative energy calibration for different particle types is of particular importance in this experiment, since ^{63}Ga is produced in reactions involving the evaporation of both α particles and protons; the analysis involves kinematic calculations using the energies of both (see

below). The relative gain of the individual phoswich detectors was checked using the monoenergetic electrons produced by a radioactive ^{207}Bi source placed at the target position. In addition, it was verified that the spectra of evaporation protons peaked at the same energy in the c.m. system in each of the phoswich detectors.

In the $^{28}\text{Si} + ^{40}\text{Ca}$ system ^{63}Ga is produced by αp evaporation. Experiments have also been performed in which the beam is replaced by ^{29}Si and ^{32}S ; in these cases ^{63}Ga is produced via the αpn and $2\alpha p$ channels, respectively. These subsequent experiments utilized phase II of the 4π phoswich array, in which approximately $\frac{2}{3}$ of the sphere was covered with telescopes. As in phase I, most of the remaining solid angle was covered by a veto detector. In the $^{29}\text{Si} + ^{40}\text{Ca}$ experiment, the cross section was measured as a function of bombarding energy between 70 and 95 MeV as a further aid to the identification process.

In addition to the identification of candidate transitions for ^{63}Ga , the charged-particle- γ coincidence data provide valuable information on possible lifetimes of isomeric states with lifetimes longer than 1 ns. The specific limits obtained depend on the energy of the γ ray, and deteriorate considerably at low energies. However, the detailed particle- γ coincidence data is extremely helpful in this regard, since known isomeric levels in neighboring nuclei can usually be isolated using suitable particle gating requirements. The capability of the system to observe isomeric states, if there are any, can thus be internally checked from the data itself. No isomeric transitions were found in ^{63}Ga ; quantitative limits obtained for individual transitions will be discussed in Sec. IV.C.

B. n - γ coincidence measurements

Once candidates for ^{63}Ga had been identified, it was determined that the most favorable reaction channel for further study was αpn evaporation following bombardment of ^{40}Ca by a 90-MeV ^{29}Si beam. The sputter ion source described by Middleton²⁰ easily produced beams of several μA of $^{29}\text{Si}^-$ from a natural-silicon cathode. Since neutron evaporation is relatively rare for compound nuclei near $N=Z$ in this mass region (statistical-model calculations using the program CASCADE²¹ predict 60% of the total fusion-evaporation cross section goes into channels in which only charged particles are evaporated) significant background reduction can be achieved using n - γ coincidences. We have constructed a modular system of neutron detectors which can be arranged in various geometries depending on the needs of an individual experiment. In the present work six of these detectors were arranged as shown in Fig. 1. Each individual detector module consists of an aluminum housing with hexagonal cross section measuring 17.1 cm face to face and 15.2 cm long. The geometry of the detectors was chosen to provide relatively high neutron efficiency and to allow close packing of the detectors, while retaining good performance in terms of light collection, timing, and pulse-shape discrimination. The cells are filled with BC501A liquid scintillator.²² An expansion reservoir allowing for temperature variations is provided.

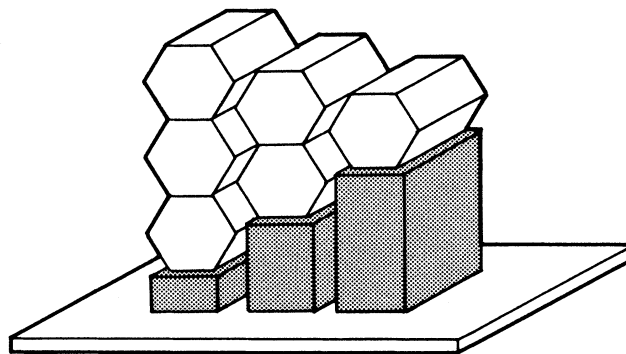


FIG. 1. Schematic diagram showing a typical arrangement of the neutron "wall." The target is vertically positioned midway between the two central neutron detectors.

The housing is optically coupled via a lucite window to a 12.7 cm diameter Amperex XP2041 photomultiplier tube (PMT) operated at negative high voltage. The PMT base is designed with a high current in the dynode chain to minimize gain shifts with count rate. The detectors were operated at rates up to approximately 50 kHz.

To increase the detection efficiency of the kinematically forward-focused neutrons, the neutron detectors were positioned in a geometry similar to that shown in Fig. 2. In this geometry the closest detectors are approximately 5 cm from the target; the front face of the detector array subtends a solid angle of nearly 2π in the laboratory system. Pulse-shape discrimination (PSD) was used to separate neutrons from γ rays. In the experiments described here temperature drifts in a preliminary version of the PSD electronics caused the n - γ separation to be somewhat less than optimum. Gamma rays in true coincidence with neutrons were enhanced relative to those in pure charged particle channels by approximately a factor of five. The neutron- γ separation was improved somewhat by attenuating γ rays in 2-cm-thick Pb shields positioned between the target chamber and the neutron detectors. The efficiency of the neutron detection system, as measured by comparing the coincidence and singles

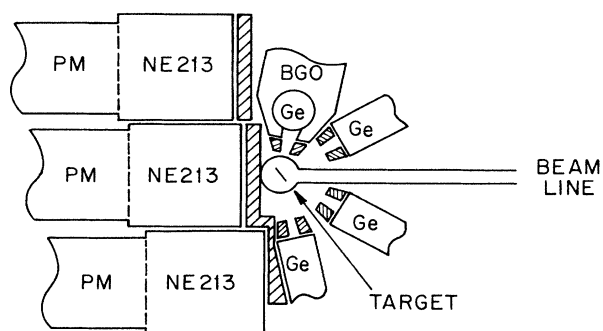


FIG. 2. Schematic diagram of the arrangement of the neutron and gamma-ray detectors for the n - γ coincidence experiment. A very similar arrangement of the neutron detectors was used for the γ -ray angular distribution measurements—see text.

yields for γ rays known to be in coincidence with a single neutron, was approximately 12%; small variations are to be expected for different reaction channels as a result of differences in the neutron spectrum shape and corresponding differences in kinematic focusing.

Gamma rays were detected using a Compton-suppressed Ge detector positioned at 90° , 120° , 135° , and 149° with respect to the incident beam. The distance from the target to the Ge detector was approximately 14 cm. An unsuppressed monitor detector was placed at a fixed position of -157° for normalization purposes. Both detectors were intrinsic n -type Ge of approximately 25% efficiency relative to a $7.62\text{ cm} \times 7.62\text{ cm}$ NaI(Tl) detector and energy resolution of 2.0 and 2.1 keV ($1332\text{ keV } ^{60}\text{Co}$), respectively. The target consisted of $500\text{-}\mu\text{g}/\text{cm}^2$ isotopically enriched ^{40}Ca evaporated on a $32\text{-mg}/\text{cm}^2$ Au backing. To reduce ^{16}O contamination, a thin layer of Au was evaporated onto the front surface; the target was transferred from the evaporator to the target chamber under vacuum.

Neutron- γ coincidence events were recorded onto WORM optical disks for subsequent off-line analysis. Even with the Pb shielding most of the counts in the neutron wall result from γ rays. Accordingly, a hardware gate was placed on the PSD signal to reject the majority of the γ rays which triggered the neutron wall. A sufficient number of these events were kept, however, in order to permit a reasonably accurate subtraction of any feedthrough from all-charged-particle channels to be performed. The entire sequence of four angles were measured three times, in random order.

C. γ - γ coincidence measurements

Most of the γ - γ coincidence information required to develop a level scheme for ^{63}Ga was obtained from an experiment in which the neutron wall described above was operated in coincidence with four 25% efficiency Ge detectors positioned in the horizontal plane at 100° and 150° on either side of the target chamber, as shown schematically in Fig. 2. The Ge γ -ray detectors were placed at a distance of 10 cm from the target in order to obtain reasonable statistics with the number of detectors available. The three unsuppressed detectors were equipped with Pb collimators with a rectangular opening of $1\text{ cm} \times 3\text{ cm}$ in order to reduce Doppler broadening. The electronic coincidence timing between the neutron and γ detectors was employed to obtain an upper limit for the lifetimes of states in ^{63}Ga . The results obtained were consistent with those found from the charged-particle- γ experiment discussed above.

Data acquisition for the n - γ - γ coincidence experiment was performed using an MBD front end and a multiprocessor farm consisting of six VME-based Motorola 68000 processors (Ref. 18). All two- or higher-fold γ - γ coincidences from the four Ge detectors were recalibrated to 1 keV/channel and sorted on line into a single $2K \times 2K$ matrix using the data-acquisition program ACQ (Ref. 23). Coincidence spectra gated on all peaks of interest previously identified in the charged-particle- γ coincidence experiment (Sec. II A) were also generated on

line, including the subtraction of an appropriate Compton background using a nearby flat region of the spectrum. All one- and two-dimensional spectra sorted on line were corrected for accidental coincidences. The on-line sorting performed did not limit the data rate, which was approximately 500 events/s.

A hardware time condition was set to reject most of the prompt events from the PSD electronics associated with γ rays. Only γ - γ events in coincidence with a PSD signal indicating a neutron and γ singles prescaled by a factor of 50 were recorded onto WORM optical disk for subsequent off-line analysis. The small fraction of feedthrough events in which a γ ray triggered the neutron wall provided the necessary information to construct accurate windows corresponding to neutrons in the two-dimensional spectra in which PSD output is plotted vs. pulse height for each scintillator.

Some additional γ - γ coincidence data was also available from the $^{28}\text{Si} + ^{40}\text{Ca}$ data described above. In that experiment phase I of the 4π phoswich array was operated in coincidence with two 25% Ge detectors placed at 90° and 135° with respect to the beam. The results obtained were consistent with those found from the n - γ - γ experiment, although the statistics were not as good.

III. DATA ANALYSIS AND RESULTS

A. Identification of ^{63}Ga

At the beginning of this work no experimental information was available on excited states in ^{63}Ga . Accordingly, several independent experiments have been used to associate in-beam γ rays with ^{63}Ga in an unambiguous way. In this section the identification process will be described in a way which at least partially reflects the history of how the experiments were done. This method of exposition is a useful guide to the use of particle- γ coincidence techniques in the identification of previously unknown nuclei which can only be produced with relatively small cross sections.

Our first attempt at identifying transitions in ^{63}Ga utilized the phase-I charged-particle- γ - γ data obtained in the $^{28}\text{Si} + ^{40}\text{Ca}$ system described in Sec. II. ^{63}Ga is produced in that system by αp evaporation. However, the spectrum of γ rays in coincidence with an α particle and a proton is dominated by feedthrough events from the much stronger $\alpha 2p$ evaporation channel in which one of the protons is missed by the phoswich array. This can occur as a result of the dead spaces between the detector modules or in front of the Ge detectors; see Ref. 17 for a complete discussion. Gamma rays from $\alpha 2p$ evaporation are also observed in coincidence with an α particle and two protons in the array; their contribution can therefore be subtracted. However, because the $\alpha 2p$ channel is very strong, such a subtraction would involve the small difference between two large numbers and would suffer from the effects of statistical fluctuations.

Accordingly, we used a method in which the energies and directions of the outgoing charged particles are used to reconstruct the kinematics of the evaporation process. The method, which is more completely described in Ref.

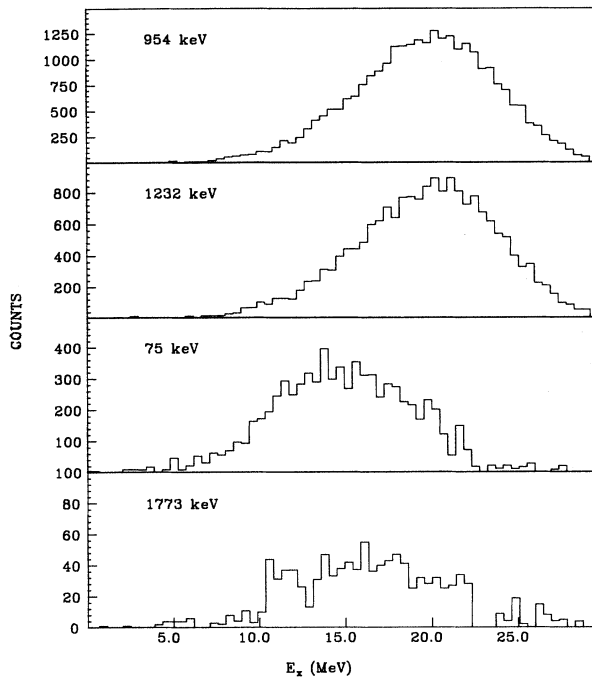


FIG. 3. Excitation energy spectra of residual systems after evaporation of one proton and one α particle. E_x is calculated from the Q value of the reaction and the energy and momentum of the evaporated charged particles detected in the 4π detector. Spectra (a) and (b) correspond to known transitions in the $\alpha 2p$ evaporation product ^{62}Zn ; spectra (c) and (d) are in coincidence with the 75 and 1773 candidate transitions in ^{63}Ga , respectively.

24, involves calculating the initial excitation energy in ^{63}Ga following αp evaporation from the ^{68}Se compound nucleus. The excitation energy E_x of the residual nucleus before γ decay is calculated from the Q value of the reaction and the energy and momentum of the evaporated particles. The latter quantities are obtained from the en-

ergies of the charged particles measured in the phoswich detectors and their directions, averaged over the angular acceptance of the detector element. If no additional particles are evaporated, this quantity will on the average be smaller than if the ultimate evaporation product is the result of additional particle evaporation, e.g., $\alpha 2p$ or αpn . Accordingly, all events involving an α particle and a proton in the 4π array were selected and a two-dimensional array of γ -ray energy vs the calculated excitation energy in ^{63}Ga was constructed. A γ spectrum gated on low values of E_x would be expected to emphasize ^{63}Ga lines over αpn lines or strong lines from $\alpha 2p$ evaporation which can feed through into the spectrum of interest as noted above. Such a cut made on the data does in fact substantially enhance lines from αp evaporation over higher multiplicity channels.

To give an idea of the effectiveness of this technique, Fig. 3 shows the calculated excitation energy spectra of the residual system after evaporation of one proton and one α particle. The upper spectra are obtained by gating on known transitions in ^{62}Zn , the $\alpha 2p$ evaporation product, while the lower spectra are gated on αp candidate transitions. As expected, the calculated excitation energy in ^{63}Ga is higher for those events in which an additional proton is evaporated. As explained more fully in Ref. 24, the resolution in the calculated excitation energy results mainly from the rather large angular acceptance ($\pm 22.5^\circ$) of the phoswich detectors. The average value of the shift in centroid between the spectra gated on transitions in ^{62}Zn and ^{63}Ga is approximately 4 MeV, which is comparable to the 2.8 MeV binding energy of the last proton in ^{63}Ga . Note also that the excitation energy spectrum corresponding to the 1773 keV transition peaks at a slightly higher value of E_x than the spectrum corresponding to the 75 keV transition. This suggests that the former transition lies above the latter in the decay scheme.

However, the improved sensitivity resulting from the cut on E_x now reveals an additional source of background which must be considered. Since there can be

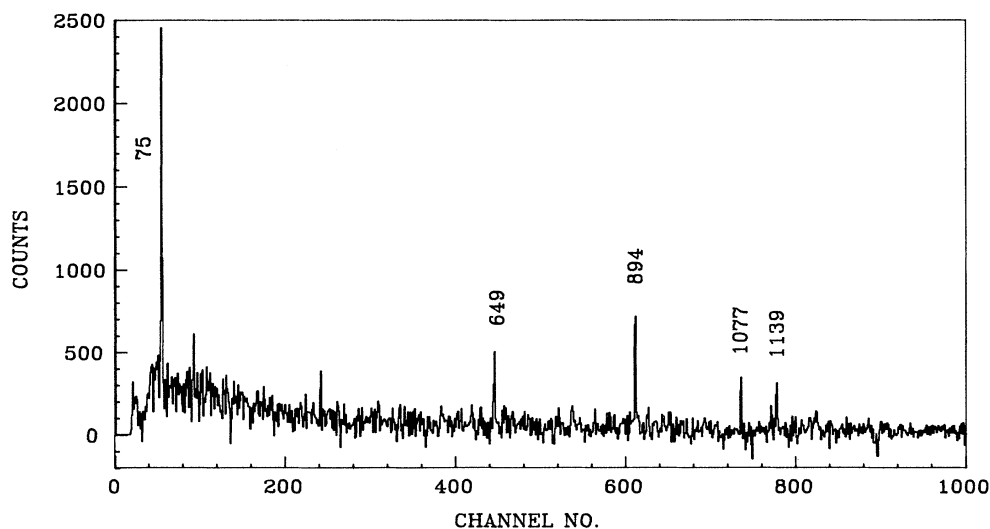


FIG. 4. Subtracted αp - γ spectrum gated on low excitation energy in ^{63}Ga from the reaction $^{28}\text{Si} + ^{40}\text{Ca}$ at 90 MeV.

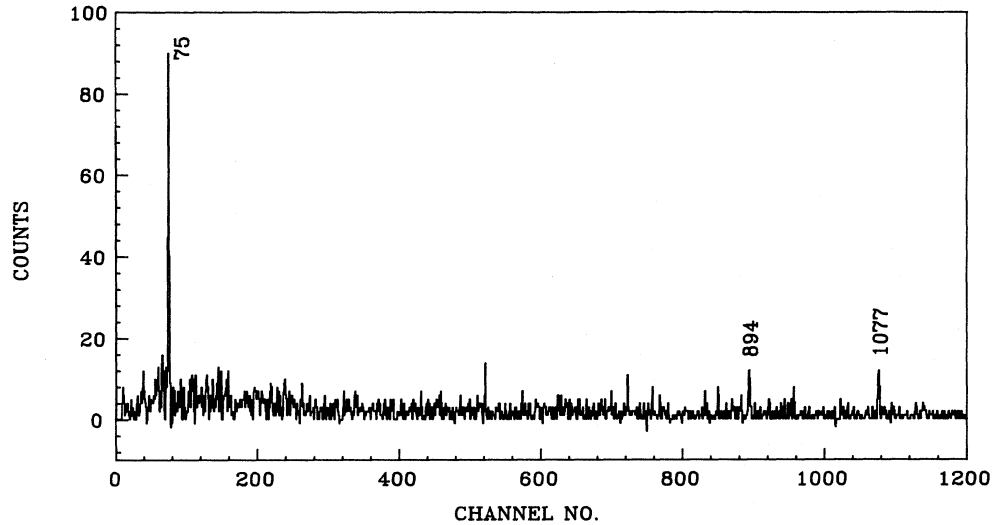


FIG. 5. The γ ray spectrum in coincidence with $2\alpha p$ from the reaction $^{32}\text{S} + ^{40}\text{Ca}$ at 96 MeV.

some overlap between $2p$ and α trajectories in the $E-\Delta E$ maps, events in which three protons are evaporated and two of them are detected by a single phoswich module can be misidentified and counted as an αp coincidence. This effect is magnified in the spectrum of interest because two protons, if treated as an α particle by the energy calibration routine, will typically correspond to a very high α -particle energy, hence a low calculated value for E_x .

The background from $3p$ evaporation is sufficiently weak that it can be accurately subtracted using spectra in which three separate protons are detected. Background lines from other channels with higher charged-particle multiplicity such as $\alpha 2p$, which have already been substantially reduced by the cut on E_x , can be subtracted in the same way. The normalization required for the subtraction was obtained using strong known lines in ^{65}Ga and ^{62}Zn for $3p$ and $\alpha 2p$, respectively. The resulting spectrum is shown in Fig. 4, and contains a series of previously unobserved γ rays. (Reactions on light-target contaminants have been ruled out with similar data taken on carbon and oxygen targets.) Finally, the excitation-energy signature (obtained from the energies and directions of the charged particles in coincidence with this cascade of γ rays) strongly implied emission of *only* two particles, leading us to assign these transitions to the αp evaporation product ^{63}Ga . A very rough estimate of the production cross section for ^{63}Ga is 5 ± 3 mb.

Confirmation of the Z identification of the product nucleus was obtained by cross bombardment using the reaction $^{32}\text{S} + ^{40}\text{Ca}$ at a bombarding energy of 96 MeV. The transitions earlier ascribed to ^{63}Ga can be identified from these data as arising from $2\alpha p x n$ evaporation; the spectrum of γ rays in coincidence with two α particles and one proton is displayed in Fig. 5.

Examination of the predictions of the statistical model for various fusion-evaporation reactions in this mass region suggested that the most prolific reaction likely to form ^{63}Ga is $\alpha p n$ evaporation in the $^{29}\text{Si} + ^{40}\text{Ca}$ system.

Further evidence in support of our assignment of candidate γ rays to ^{63}Ga has been obtained by studying the latter reaction as a function of bombarding energy using charged-particle- γ coincidence techniques. Figure 6 shows the intensity of strong γ rays of representative two-, three-, and four-particle evaporation channels as a function of the beam energy. The quoted cross sections were obtained from the measured yields using detection efficiencies determined as discussed in Sec. V below. The excitation function for the 75-keV γ ray, which in this system should be associated with $\alpha p n$ evaporation, is very similar to that observed for the previously established

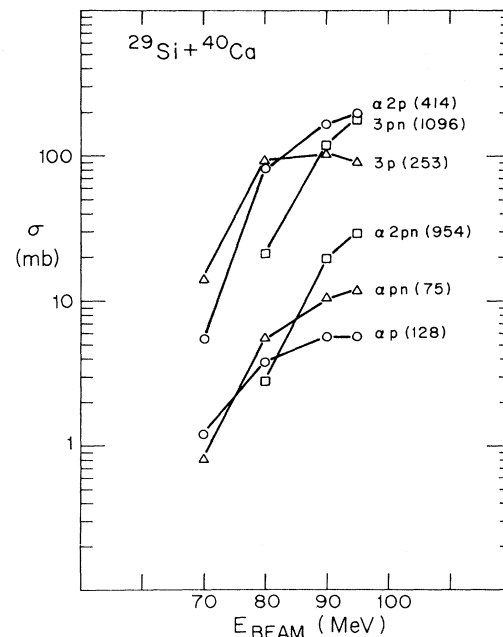


FIG. 6. Excitation function for the $^{29}\text{Si} + ^{40}\text{Ca}$ system determined from the specified transitions (in keV).

$\alpha 2p$ channel. This observation is consistent with the fact that all of the ^{63}Ga candidate lines are observed in coincidence with neutrons in the $^{29}\text{Si} + ^{40}\text{Ca}$ system. All of the information given here unambiguously establishes the association of the new group of γ rays with ^{63}Ga .

B. Analysis of n - γ angular distribution measurements

Despite the n - γ coincidence requirement, all transitions in ^{63}Ga were found to be only partially resolved from γ rays of other neighboring nuclei also populated via neutron evaporation, generally with considerably larger cross sections. The peak areas were thus obtained by fitting portions of the γ spectrum around the peaks of interest, large enough to allow for adequate background determination, using a least-squares minimization routine assuming a peak shape of a Gaussian plus exponential tail. The peak shape was determined as a function of energy using isolated peaks in strongly produced channels and then held approximately constant in the fitting process. A first-order angle-to-angle normalization was derived from several strong peaks in the monitor spectrum. Comparison of the intensity of the reference peaks with the integrated charge suggested, however, that some corrections, possibly related to small motions of the beam spot during the measurements, were necessary. An empirical correction to the normalization was constructed (at the $\pm 5\%$ level) using both the angular distribution of the strong 547-keV line from Coulomb excitation of the Au target backing²⁵ and from strong transitions in the $2pn$ evaporation product ^{66}Ge , for which there exist published²⁶ angular distributions obtained under conditions similar to those of the present work. Where the different methods of normalization disagreed, the experimental error on the yield as a function of angle was increased to accommodate the difference. In the case of most of the transitions in ^{63}Ga , the normalization uncertainties are smaller than the errors arising from counting statistics and peak fitting. For low-energy transitions with relatively good statistics, such as the 191-keV line in ^{65}Ga (for which new information was also obtained—see below) and the 75-keV line in ^{63}Ga , some additional uncertainty results from the fact that if the position of the beam spot is subject to small changes during the measurements the corrections for γ -ray absorption in the chamber walls, which were made using radioactive sources placed at the nominal target position, may not be completely accurate. In the case of the 75-keV transition, where this problem would be most acute, an additional normalization was used in which it was assumed that the yield of x rays from the Au target backing is isotropic. This procedure should cancel any differences in absorption resulting from motion of the beam spot. The results of this latter procedure were averaged with those obtained with the normalization(s) described above, and the quoted errors encompass all of the methods used. Finally, in the case of the 191-keV transition in ^{65}Ga , a small correction was made for feedthrough of a 190.2-keV transition in ^{66}Ga into the n - γ coincidence spectra using the published²⁷ angular distribution. (Note that there is also a line from Coulomb excitation of the Au target backing

which is unresolved from the 191-keV line; because of its low associated γ ray multiplicity it is efficiently rejected by the n - γ coincidence requirement and makes a negligible contribution to the measured yield. Similarly, a 190.4-keV transition in the αp product ^{64}Ga ²⁸ has negligible yield and is not a problem.)

The angular distribution coefficients A_k were obtained by fitting the experimental data to a sum of Legendre polynomials:

$$W(\theta) = \sum_{k=0,2,4} Q_k A_k P_k(\cos\theta),$$

where $W(\theta)$ is the normalized γ -ray intensity at the angle θ , measured with respect to the beam direction. The Q_k are attenuation coefficients due to the finite solid angle of the detectors. Note that, strictly speaking, the coefficients Q_k can only be defined for cylindrically symmetrical detectors. We have assumed a cylindrically symmetrical acceptance of half-angle 9.5° defined by the aperture of the Compton suppressor,²⁹ and have made a small correction to account for the finite thickness of the detector. Because the distance of the detector to the target is considerably larger than the characteristic dimensions of the detector, the effect of these approximations on extracting correct angular distribution coefficients A_2/A_0 and A_4/A_0 is negligible. The results of the angular distribution analysis are shown Table I. Intensities are listed as the A_0 coefficient of the Legendre polynomial fit. The intensity of the 75.4-keV transition has been corrected for internal conversion (see Sec. III). Errors in the intensities are derived from the errors from the angular distribution fit to the peak areas. The small cross section of ^{63}Ga compared to other channels involving neutron evaporation, in particular ^{65}Ga ($3pn$) and ^{66}Ge ($2pn$), and the complex structure of the involved peaks gives rise to the rather large errors quoted in Table I.

C. Analysis of γ - γ coincidences and directional correlation with oriented nuclei (DCO) ratios

The n - γ - γ coincidence data consist of approximately 50 million events, and reside on one side of a WORM optical disk. Replay of the data, which can be done for the entire data set without operator intervention, consists of reducing the measured pulse heights from the different Ge detectors to a common calibration (1 keV/channel), making a software cut on the pulse-shape discriminator output to sharpen n - γ discrimination, and histogramming the resulting $(E_{\gamma_1}, E_{\gamma_2})$ pairs in a $2K$ by $2K$ array. Accidental coincidences, which were dominated by events in which a neutron and one of the γ rays were in true coincidence, were corrected for using events from appropriate regions of the two dimensional $(\Delta T_i - \Delta T_j)$ space, where ΔT_j is the output of the time-to-amplitude converter (TAC) measuring the time between the neutron detector output and that of the γ detector labeled by j . The timing for the different neutron detector modules was lined up in hardware; no additional software correction was made. To illustrate the quality of the γ - γ coincidence data, two typical gated γ spectra are shown in

TABLE I. Relative intensities and angular distributions of γ rays in ^{63}Ga

E_γ (keV) ^a	E_x (keV)	I_γ	a_2	a_4
75.4	75.4	141(12) ^b	0.11(6)	0.09(7)
624.6	624.6	12(5)	0.18(12)	0.13(16)
649.1	4729.3	60(5)	0.21(11)	-0.21(15)
894.1	2046.7	142(6) ^c	0.28(6) ^c	-0.14(7) ^c
894.1	2940.8	c	c	c
1077.2	1152.6	100(5)	0.26(7)	-0.11(10)
1139.4	4080.2	67(4)	0.34(9)	-.21(14)
1208.8	7710.9	23(8)	0.32(30)	-0.12(41)
1422.0	2046.7	8(4)	d	d
1772.8	6502.1	55(5)	-0.17(9)	-0.21(13)

^aGamma-ray energies are uncertain to ± 0.3 keV, except for the 624.6-, 1208.8-, and 1422.0-keV transitions, for which the errors are ± 0.5 keV.

^bCorrected for internal conversion ($\alpha = 0.28$)

^cIndistinguishable doublet. Intensity and a_2 and a_4 given are for the sum.

^dInsufficient intensity to obtain a meaningful angular distribution.

Figs. 7 and 8: one in coincidence with the 894-keV doublet (Fig. 7) and one gated on the 1139-keV transition (Fig. 8).

Additional information relevant to the determination of multiplicities was obtained from DCO ratios obtained from the n - γ - γ data. The required ratio may be obtained from the definition:

$$R_{\text{DCO}} = \frac{W(\gamma_1 \text{ at } 100^\circ, \gamma_2 \text{ at } 150^\circ)}{W(\gamma_2 \text{ at } 100^\circ, \gamma_1 \text{ at } 150^\circ)}, \quad (1)$$

where $W(\gamma_1 \text{ at } 100^\circ, \gamma_2 \text{ at } 150^\circ)$ is the yield of γ_1 at 100° in coincidence with γ_2 at 150° . To generate the DCO ratios, events from the n - γ - γ coincidence data in which the

two- γ rays were detected at different angles were sorted into a two dimensional array. Projection from this array thus gave the required yields from which R_{DCO} could be calculated. Of the six possible detector pairs only four are useful for this procedure; in addition, because the yields at individual angles must be examined, the statistics are considerably worse than in the gated spectra without this requirement. The results are presented in Table II. The middle column shows the interpretation given to the DCO results in the light of all of the available experimental evidence. In general, a pair of stretched quadrupole transitions gives a DCO ratio of unity. If γ_1 is a quadrupole transition and γ_2 is a dipole transition, R_{DCO} is less than one, whereas if γ_1 is a dipole

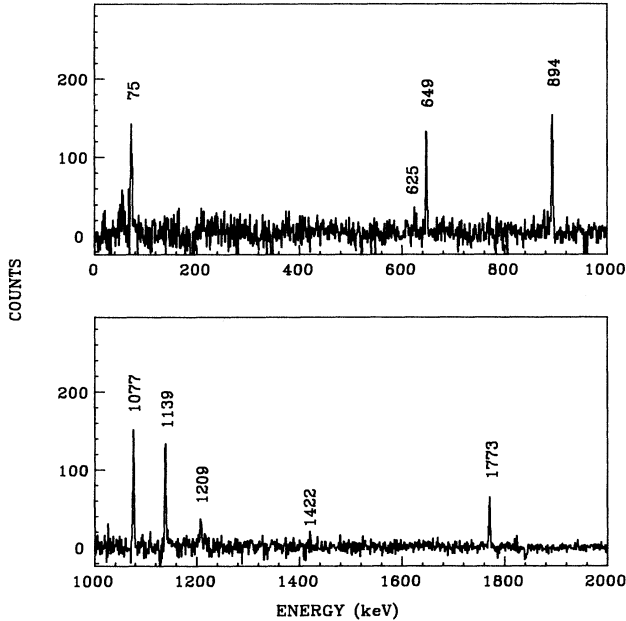


FIG. 7. The γ -ray spectrum in coincidence with neutrons gated on the 894-keV doublet in ^{63}Ga .

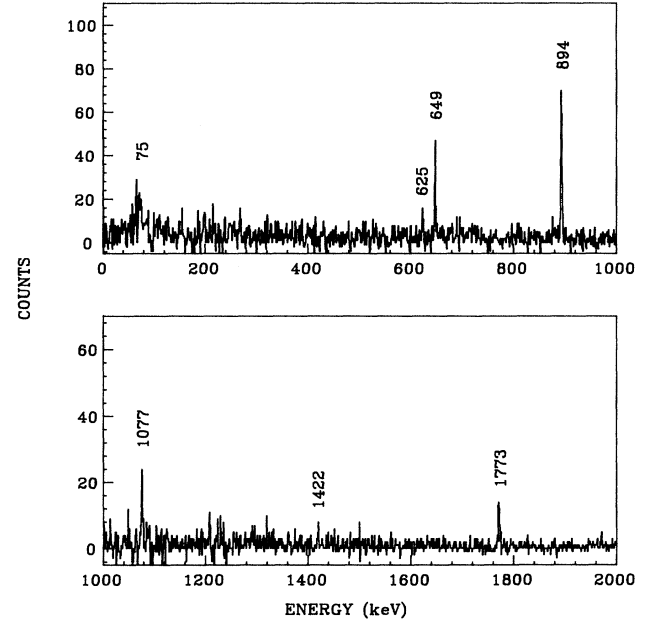


FIG. 8. The γ -ray spectrum in coincidence with the 1139-keV transition in ^{63}Ga .

TABLE II. Experimental DCO ratios for transitions in ^{63}Ga

$E_{\gamma 1}$	$E_{\gamma 2}$	Multipolarity	R_{DCO}
1077.2	75.4	(Q,D)	0.6(2)
894.1	75.4	(Q^* ,D) ^a	0.6(2)
894.1	1077.2	(Q^* ,Q)	1.0(1)
1139.4	1077.2	(Q,Q)	1.3(3)
1139.4	894.1	(Q, Q^*)	1.0(1)
649.1	1139.4	(Q^* ,Q)	0.9(1)
649.1	894.1	(Q^* , Q^*)	0.9(1)
1772.8	649.1	(D, Q^*)	3.3(3)
1772.8	1139.4	(D,Q)	2.3(3)
1772.8	894.1	(D, Q^*)	1.9(3)
1208.8	1772.8		0.8(4)
1208.8	649.1	b	1.8(4)
1208.8	1139.4	b	1.6(4)

^a The notation Q^* refers to transitions believed to be either quadrupole or dipole with $\Delta J = 0$.

^b Statistics insufficient for a firm conclusion, but possibly suggestive that 1208.8-keV γ ray has dipole character.

transition and γ_2 is a quadrupole R_{DCO} is greater than one. A $\Delta J = 0$ dipole transition gives results similar to a stretched $E2$; at the level of precision of the present data they can not in general be distinguished. The notation Q^* in Table II denotes a transition which is believed on the basis of all of the available evidence to be either quadrupole or a $\Delta J = 0$ dipole—see Sec. IV.

D. New information on ^{65}Ga

In addition to the γ rays identified in ^{63}Ga , the present set of experiments permits an interesting reexamination of some low-lying levels in ^{65}Ga . In the $^{29}\text{Si} + ^{40}\text{Ca}$ system ^{65}Ga is produced by $3pn$ evaporation and thus is present in both the charged-particle- γ and n - γ coincidence spectra. The analysis procedures were in all cases similar to those described above; both angular distributions and DCO ratios were extracted. In the $^{28}\text{Si} + ^{40}\text{Ca}$ system ^{65}Ga is formed by $3p$ evaporation. We have also obtained DCO ratios from an independent set of data taken in this system at a bombarding energy of 90 MeV. This earlier experiment is described in Ref. 1. Briefly, γ - γ coincidences were measured in two Ge detectors (unsuppressed) placed at angles of 90° and 135° with respect to the beam gated on the output of an early version of the 4π charged-particle detector used in the present work. For the present purpose we focus on events in which either two or three protons were observed in coincidence with two γ rays. (Because the three-particle efficiency of the phase I 4π detector was relatively low, events where only two of the three protons were detected were included to improve the statistics.) In this case the DCO ratio is defined as in Eq. (1) except that the detector angles are 90° and 135° instead of 100° and 150° .

IV. THE LEVEL SCHEME OF ^{63}Ga

A. Low-lying negative-parity states in $^{63,65}\text{Ga}$

Prior to the current investigation no information about excited states in ^{63}Ga had been reported. Previous work

on its radioactive decay established the half-life and imposed a restriction of the possible spin and parity of the ground state. The first identification of ^{63}Ga by Nurmi and Fink (Ref. 30) in 1965 was based on radiochemical separation and the half life of its β decay was measured to be 33 ± 4 sec. In a subsequent investigation by Dulfer *et al.* (Ref. 15), γ transitions from excited states in ^{63}Zn following the β decay of ^{63}Ga were identified. Their half life measurement yielded a value of $T_{1/2} = 31.4 \pm 0.8$ sec and is in good agreement with the previous work. Observation of allowed β decay to the firmly established³¹ $\frac{3}{2}^-$ ground state and $\frac{5}{2}^-$ first excited state in ^{63}Zn restrict the spin and parity of the ground state of ^{63}Ga to $J^\pi = \frac{3}{2}^-$ or $\frac{5}{2}^-$.

In establishing the level scheme of ^{63}Ga , the systematics of nearby nuclei can provide useful guidance. The neighboring odd isotopes ^{65}Ga and ^{67}Ga have spin and parity of $J^\pi = \frac{3}{2}^-$ for their respective ground states,^{11,9} suggesting that the odd proton occupies the $2p_{3/2}$ subshell. In both cases the first excited state has $J^\pi = \frac{5}{2}^-$ and its decay to the ground state is the strongest transition in the level scheme. Correcting for internal conversion and accounting for the doublet nature of the 894-keV transition, as discussed below, the 75.4-keV γ ray is the strongest transition found in ^{63}Ga in the present work. In addition, the excitation curve observed for this γ ray shows the smallest increasing slope with energy of all the candidates observed, consistent with placing it at the bottom of the decay scheme. Its nearly isotropic angular distribution is consistent with a predominantly dipole transition with a small (approximately 6%) quadrupole admixture, as is the observed DCO ratio with the 1077-keV transition. Given the systematics and the fact that heavy-ion fusion evaporation reactions selectively populate yrast states, we give a $J^\pi = \frac{3}{2}^-$ assignment to the ground state of ^{63}Ga preference over $J^\pi = \frac{5}{2}^-$ and assign $J^\pi = \frac{5}{2}^-$ to the first excited state.

All γ rays identified in the charged-particle- γ data to be in ^{63}Ga are in coincidence with each other. Typical gated spectra are shown in Figs. 7 and 8. Thus, placing

all these transitions in one cascade, the ordering should be determined by the measured intensity of the peaks. However, the situation is somewhat complicated by the fact that the 894.1-keV transition is a doublet. As seen in Fig. 7, the spectrum in coincidence with the 894.1-keV γ ray reveals a strong peak with a centroid that is, within experimental errors, identical to the centroid of the gating transition. No noticeable broadening of this γ ray is observed in the singles spectra, making it impossible to resolve the doublet structure experimentally. The existence of this indistinguishable doublet at 894.1 keV makes it impossible to order the levels purely on the basis of the intensities of the transitions.

Some additional information is provided by the existence of two weak peaks at 624.6 and 1422.0 keV in the spectrum in coincidence with the 1139.4-keV transition (see Fig. 8), adding up to 2046.6 keV. This is, within the experimental uncertainties, equal to the sum of the 75.4 + 1077.2 + 894.1 keV transitions. A gate on the 625-keV peak contains peaks at 649, 894, 1139, 1422, and 1773 keV, although some of these have intensities very near the limit of sensitivity of the data. In the spectrum in coincidence with the very weak 1422.0-keV γ ray the only peaks distinguishable from the background are at 625 keV, the strongest transition, and 678, 894, 956 and 1139 keV. The 678- and 956-keV γ rays have not been placed at present. Most importantly, neither the 75.4- nor the 1077.2-keV γ rays were observed in either of the spectra gated on the 624.6- or the 1422.0-keV transitions; the spectrum gated on the 625-keV transition is shown in Fig. 9. Thus the 624.6- and 1422.0-keV γ rays represent an alternate decay path from the initial state of the 75-1077-894 keV cascade. Note that in ordering the 1077- and 894-keV transitions as we have (see Fig. 10) we have

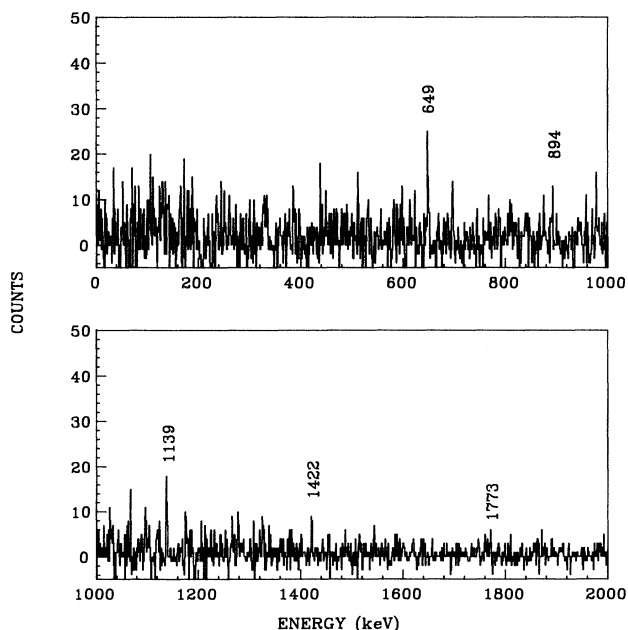


FIG. 9. The γ -ray spectrum in coincidence with neutrons gated on the 625-keV transition.

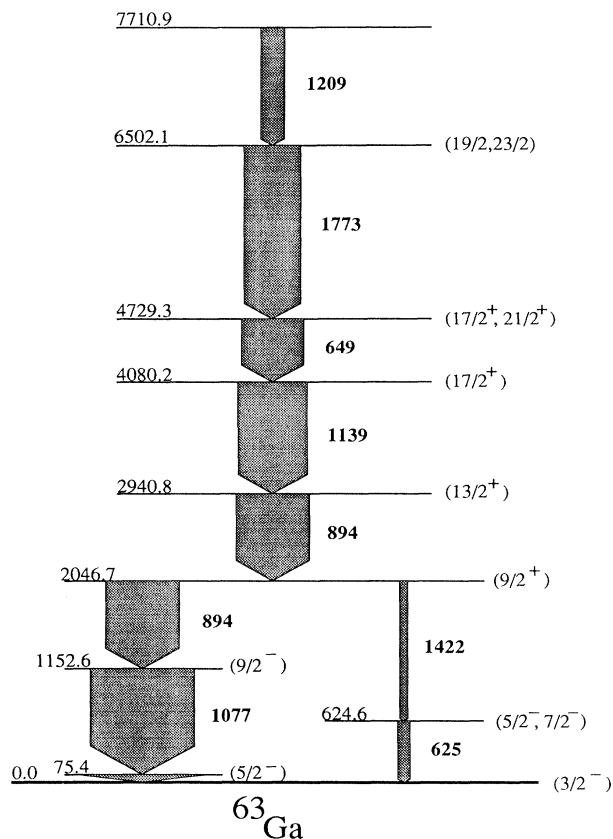


FIG. 10. The energy-level scheme for ^{63}Ga obtained from the present work. Transition and level energies are in keV. Note that the order of the 625- and 1422-keV transitions is uncertain—see text.

assumed an approximately equal division of intensities between the two members of the 894-keV doublet. This is consistent with the expected yrast feeding pattern and with the systematics of neighboring nuclei. In addition, both the excitation curve data and the excitation energy measurements are consistent with placement of the 894-keV transition(s) near the bottom of the level scheme.

The angular distribution of the 1077.2-keV transition is consistent with $\Delta J=2$ and, combined with the assumption of the yrast nature of the initial state, suggests $J^\pi = \frac{9}{2}^-$. (Negative parity is strongly favored by the limit on the lifetime obtained in the present work; an $M2$ transition would have a strength greater than 0.6 W.u.) The $\frac{9}{2}^-$ assignment is consistent with the DCO ratio for the 75–1077 keV sequence. The angular distribution of the 75-keV transition is nearly isotropic. Since under plausible assumptions about the alignment of the $\frac{5}{2}^-$ state a pure $M1$ transition would be expected to have an appreciably negative a_2 coefficient, this observation suggests the possibility of an $E2$ admixture. In fact, analysis of the γ -ray angular distributions (see below) does imply a small $E2$ admixture; the multipole mixing ratio $\delta(E2/M1)$ for the 75-keV transition is found to be equal to -0.25 ± 0.05 . This mixing ratio implies an internal conversion coefficient of 0.28. When corrected for this

amount of internal conversion, the ratio of the intensities of the 1077- and 75.4-keV transitions is found to be 0.71 ± 0.07 , nearly equal to the corresponding ratio of 0.68 ± 0.07 found in ^{65}Ga (see Ref. 11).

For the very weak parallel decay branch out of the $E_x = 2046.7$ -keV state, both the level ordering and the spin of the intermediate state are difficult to establish on the basis of the present evidence. Here we offer only some speculations regarding this portion of the level scheme. The intensity of the 624.6-keV transition is slightly greater than the 1422.0-keV γ ray and supports the order suggested in Fig. 10. However, all the evidence combined is still clearly marginal and we consider the ordering of the 624.6- and 1422.0-keV transitions to be tentative. The lifetime limits obtained in the present work restrict the multipolarity of both transitions in the side branch to be less than or equal to 2. The assumption that the $E_x = 2046.7$ keV $\frac{9}{2}^+$ state (discussed below) is the lowest-energy positive-parity state, as is the case in the other odd-A Ga isotopes, requires $J^\pi = \frac{5}{2}^-$ or $\frac{7}{2}^-$ for the intermediate state of the weak side branch. The angular distribution of the 625-keV transition is mildly suggestive of a stretched $E2$ decay, implying $J^\pi = \frac{7}{2}^-$ for the intermediate state, but could also be consistent with a mixed $E2/M1$ transition as would occur for a $\frac{5}{2}^-$ assignment. We note further that a $\frac{5}{2}^-$ assignment to the intermediate state favors an excitation energy of 625 keV; with the lifetime limit obtained in the present work (see below) the $B(M2)$ for the $\frac{9}{2}^+ \rightarrow \frac{5}{2}^-$ transition would be 0.013 or 0.81 W.u. for $E_\gamma = 1422$ and 625 keV, respectively. The former value is quite consistent with the $B(M2)$ s observed for analogous transitions in this mass region, while the latter is not. If the spin of the intermediate state is taken as $\frac{7}{2}^-$, then a weak argument in favor of the higher possible excitation energy can be made by noting that the ratio of the $B(E1)$ s connecting the $\frac{9}{2}^+$ to the $\frac{9}{2}^-$ and $\frac{7}{2}^-$ levels in the neighboring nuclei ^{65}Ga and ^{67}Ga is 4.8 and 2.7, respectively.^{11,9} The corresponding ratios for placement of the $\frac{7}{2}^-$ level at $E_x = 625$ or 1422 keV are 40.2 and 3.4, respectively. If one assumes that the $B(E1)$ s should be similar, a somewhat questionable assumption in view of the fact that $E1$ transitions are normally quite retarded, then $E_x = 1422$ keV for the $\frac{7}{2}^-$ level would be preferred.

We now turn to an analysis of the γ -ray angular distributions for the $\frac{9}{2}^- \rightarrow \frac{5}{2}^- \rightarrow \frac{3}{2}^-$ cascade in $^{63,65}\text{Ga}$. As noted above, the mixing ratio reported in Ref. 11 for the 191-keV $\frac{5}{2}^- \rightarrow \frac{3}{2}^-$ transition in ^{65}Ga , $\delta_{191} = 0.7 \pm 0.3$, taken with the published limit on the lifetime, $T_{1/2} < 0.7$ ns, implies a lower limit on the $B(E2)$ of 28 W.u., which would correspond to a reasonably collective transition. This result is quite interesting, since in the heavier Ga isotopes the lowest $\frac{5}{2}^-$ state is of predominantly single-particle character. In $^{67,69,71}\text{Ga}$ the $B(E2)$ s for this transition are, respectively, 0.41 ± 0.04 , 0.49 ± 0.07 , and < 0.19 W.u.^{8,9,10} The spectroscopic factors for proton transfer to these levels from the ground state of the corresponding Zn isotopes are all large.³² In these latter nuclei it is the second $\frac{5}{2}^-$ level, occurring at an excitation ener-

gy of about 1 MeV, which has a collective $E2$ decay. These higher states are presumably well described as a proton in the fp -shell coupled to the lowest 2^+ state of the neighboring Zn core. As expected, these latter states are weakly excited in single nucleon transfer reactions.³² The expected single particle nature of the lowest $\frac{5}{2}^-$ level is also supported by an earlier measurement of the $E2/M1$ mixing ratio of the 191-keV transition in ^{65}Ga by Nemashkalo *et al.*, who analyzed γ - γ angular correlations following proton capture using the statistical model¹⁴ and found a mixing ratio consistent with a pure $M1$ transition.

In order to obtain the $E2/M1$ mixing ratio from the experimentally measured angular distribution of the $\frac{5}{2}^- \rightarrow \frac{3}{2}^-$ transition the required magnetic substate population can be deduced from the preceding $\frac{9}{2}^- \rightarrow \frac{5}{2}^-$ transition, assuming the latter to be of pure multipolarity. In the actual fits the substate distribution of the $\frac{9}{2}^-$ level was parameterized as a Gaussian, $P(M) = \text{const} \times e^{-M^2/2\sigma^2}$; for each value of the mixing ratio, the width parameter σ was varied to produce the best fit. The goodness of fit parameter χ^2/ν is plotted vs $\phi = \tan^{-1}\delta$ for ^{63}Ga and ^{65}Ga in Figs. 11(a) and 11(b), respectively. In both cases minima are obtained for a small value of δ corresponding to a nearly pure $M1$ transition and for a larger positive value of δ for which $E2$ decay dominates. (Note that because the experimental errors in the case of ^{65}Ga are predominantly systematic, resulting from normalization and absorption uncertainties, the numerical value of χ^2/ν is not meaningful.) The known lifetime limit for the $\frac{5}{2}^-$ state in ^{65}Ga argues strongly against the

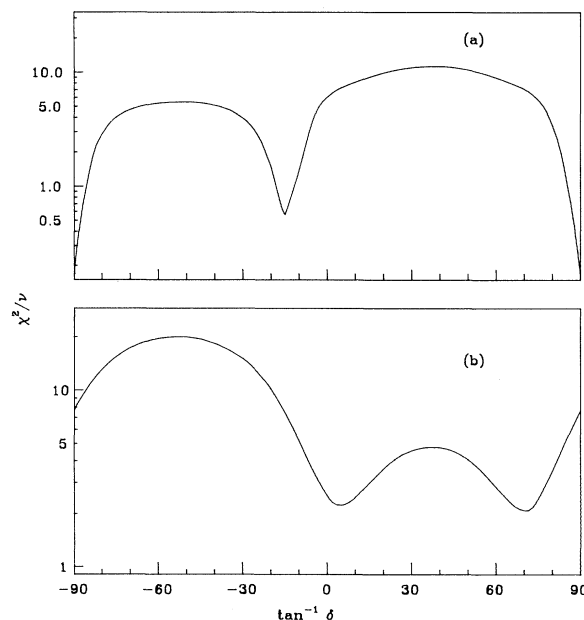


FIG. 11. (a) χ^2/ν as a function of $\phi = \tan^{-1}\delta$ for the 1077-75 keV cascade in ^{63}Ga . (b) Same for the 1096-191 keV cascade in ^{65}Ga .

larger mixing ratio. The fit with the larger mixing ratio shown in Fig. 11(b), corresponding to $\delta \approx 2.7$, would imply a $B(E2)$ of over 150 W.u. The width parameter σ from the fits was found to be the same in the two nuclei: $\sigma = 1.8 \pm 0.3$ for ^{65}Ga and $\sigma = 1.8 \pm 0.3$ for ^{63}Ga . In the former case σ could be extracted for a number of transitions as a function of excitation energy. The characteristic distribution width σ/J decreases as the excitation energy increases. For the $\frac{5}{2}^-$ state in ^{65}Ga , the measured width of the distribution corresponds to an attenuation coefficient $\alpha_2 = 0.61 \pm 0.13$, in good agreement with the value 0.60 used for the analysis of the same transition in Ref. 11. The best fits to both transitions in the cascade are shown for both nuclei in Fig. 12 as solid lines. The dashed curve in Fig. 12(d) is calculated using $\delta_{191} = 0.7$ but keeping σ fixed at 1.8. This fit is clearly in disagreement with the data; it can be improved somewhat by increasing σ , but at the expense of making the fit to the preceding 1096-keV transition worse. We therefore adopt the value corresponding to the smaller mixing ratio, $\delta = 0.09 \pm 0.08$. In the case of ^{63}Ga the best fit, corresponding to $\delta = -0.25 \pm 0.05$, is shown as a solid line [Fig. 12(b)]. The dashed curve shows the expected angular distribution for a pure $M1$ transition with σ fixed at 1.8. A slightly better fit can be obtained for a much larger value of σ , but again at the expense of worsening

the fit to the preceding 1077-keV transition. The data thus suggest a small $E2$ admixture, but given the possible systematic nature of the errors at this low γ -ray energy, the experimental error given on the mixing ratio should be considered with caution.

The results concerning δ_{191} deduced from the angular distributions above are corroborated by the DCO ratios measured for both the $^{28}\text{Si} + ^{40}\text{Ca}$ charged-particle- γ - γ data and the $^{29}\text{Si} + ^{40}\text{Ca}$ n - γ - γ data. These have been interpreted assuming a value of σ consistent with that obtained from the angular distribution measurements. For the 191-keV transition, a mixing ratio of 0.09 predicts DCO ratios of 0.563 and 0.493 for the results obtained with the $3p$ and $3pn$ reactions respectively. (Recall that the Ge detectors were placed at different angles in the experiments in which these two reactions were used.) These may be compared with the experimental values of 0.65 ± 0.04 and 0.48 ± 0.03 ; the agreement is reasonable. A mixing ratio of 0.7, on the other hand, would predict DCO ratios of 0.412 and 0.320 for the two measurements, in significant disagreement with observation. In the case of the 75-keV transition in ^{63}Ga , the DCO measurements do not distinguish between the best-fit mixing ratio obtained and that for a pure $M1$ transition. It thus appears that neither the angular distribution nor the DCO measurements support the value $\delta = 0.7$ found for the 191-keV transition in ^{65}Ga in Ref. 11. We conclude that in ^{65}Ga the vast majority of the available experimental evidence is consistent with a $\frac{5}{2}^- \rightarrow \frac{3}{2}^-$ transition that is predominantly $M1$. There does not appear to be any evidence for a sudden appearance of collectivity in this transition at $N=34$. With this said, however, the present data for $N=32$ ^{63}Ga do suggest the presence of a significant $E2$ admixture. Given the lifetime limit obtained in the present work ($T_{1/2} < 25$ nsec—see below) the mixing ratio obtained implies a lower limit on the $B(E2)$ for the 75-keV transition of approximately 20 W.u. Unfortunately, in view of the systematic uncertainties associated with the measurement of the angular distribution of the 75-keV transition, this indication must be regarded as preliminary. Additional experimental work will be required to establish with certainty whether the trend is in fact broken at $N=32$.

B. Higher-lying states in ^{63}Ga

The state at $E_x = 2046.7$ keV is depopulated by the 894- and 1422-keV transitions. The combined angular distribution for the 894-keV doublet is consistent with $\Delta J = 0, 2$. No multipolarity information for the 1422-keV γ ray can be obtained from the angular distribution data due to its lack of intensity. However, the upper limit of 2 nsec for the lifetime of this level (see Sec. V A below) rules out any multipolarity greater than 2 for the 1422-keV transition. It should be noted that the excitation energy of the $g_{9/2}$ orbital in neighboring nuclei in this mass region is around 2 MeV, hence the existence of a $\frac{9}{2}^+$ level is expected from the systematics. We therefore favor a $J^\pi = \frac{9}{2}^+$ assignment for the initial state of the 894- and 1422-keV transitions.

The ordering of the subsequent level scheme is based

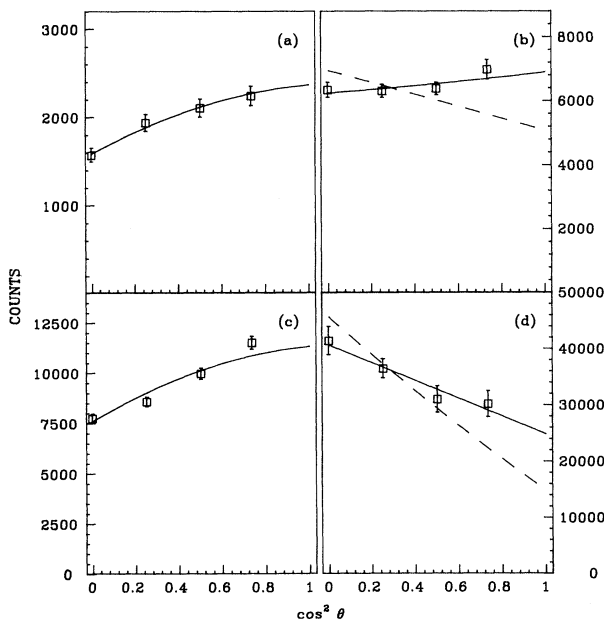


FIG. 12. (a) Experimental angular distribution of the 1077-keV transition in ^{63}Ga ; the solid line assumes a $\frac{9}{2}^- \rightarrow \frac{5}{2}^-$ transition—see text; (b) experimental angular distribution of the 75-keV γ ray in ^{63}Ga : the solid and dashed lines correspond to mixing ratios of -0.25 and zero, respectively—see text; (c) experimental angular distribution of the 1096-keV transition in ^{65}Ga —see text; (d) angular distribution of the 191-keV γ ray in ^{65}Ga —the solid curve corresponds to the best fit ($\delta = 0.09 \pm 0.08$), while the dashed curve corresponds to the value $\delta = 0.7$ found in Ref. 11.

on the relative intensities, since all the remaining transitions are in coincidence with each other. However, due to the doublet nature of the 894.1-keV transition the individual intensities can only be estimated, and thus a different placement of the second 894.1-keV γ ray higher up in the decay scheme cannot be ruled out. The ordering of the 649.1- and 1772.8-keV transitions has to be also regarded as tentative due to their rather similar intensities. The lifetime limit obtained for the state emitting the 649-keV γ ray rules out $M2$ multipolarity for this transition. Our proposed level scheme is somewhat favored by the systematics of the neighboring odd isotopes and is consistent with the observed intensities. Spin assignments are based on the measured angular distributions and DCO ratios, the usual assumptions about fusion-evaporation reactions feeding predominantly yrast states, and comparison with the systematics of neighboring nuclei.

C. Search for isomeric levels in ^{63}Ga

The existence of isomers in this mass region has proven to be an effective tool for assignment of spins and parities. The $N = Z + 1$ systems ^{65}Ge and ^{69}Se both have isomeric $\frac{9}{2}^+$ states which decay by $M2$ transitions to low-lying $\frac{5}{2}^-$ states.^{1,6,7} In ^{63}Ga the spin assignments suggested in Sec. IV would not permit observation of such a decay because a low-lying $\frac{9}{2}^-$ state allows the transition from positive- to negative-parity yrast states to be made via an $E1$. However, as isomers can always result from decays which are inhibited for structural reasons, we have carried out a systematic search for long-lived levels in ^{63}Ga .

The ΔE signal from the plastic component of the phoswich detectors in the 4π array provides a good start signal for the direct measurement of nuclear lifetimes by electronic timing. The accessible region of lifetimes depends mainly on the γ -ray energy, since the timing is determined by the response of the Ge detector which is strongly energy dependent, particularly at low energies. Using our setup it is possible to search for isomers in the lifetime range from 1–2 nsec to several μsec using this technique. In the present case the charged-particle- γ coincidence data taken at a bombarding energy of 90 MeV in the $^{29}\text{Si} + ^{40}\text{Ca}$ system were used. In the analysis all γ rays observed in coincidence with an α particle and a proton were placed in a two-dimensional array with axes labeled by ΔT and E_γ , where ΔT is the output of a time-to-amplitude converter (TAC) measuring the time between the timing signal from the charged-particle array and the corresponding signal from the Ge detector. The potential sensitivity of the technique may be estimated by examining the TAC spectrum for lines known to be prompt. The slope of the prompt resolution function obtained in this way ranges from approximately 20 nsec at $E_\gamma = 41$ keV to 1.2 nsec at $E_\gamma = 1534$ keV.

Time spectra for all of the lines placed in ^{63}Ga for which adequate statistics were available were examined to search for any delayed components which might be present. None were found. In each case an upper limit was set in an approximate way by reference to the prompt resolution function for a similar value of E_γ .

The limit obtained for the first excited state at $E_x = 75.4$ keV is a half-life of approximately 25 nsec. (This transition occurs in a region of γ ray energy where the timing is deteriorating rapidly with energy.) The limits are much better at higher energies. For example, limits on the lifetimes of the γ rays at 894, 1077, 1140, and 1772 keV are, respectively, 1.7, 2.0, 1.8, and 1.3 nsec. We note that the 1077-keV line may contain some contamination from a line of the same energy in ^{65}Ga which can appear in the spectrum of interest from events in which two protons are incorrectly identified as an α particle. Similarly the γ rays at 649 and 1208 keV are somewhat affected by feedthrough from neighboring lines in the $\alpha 2p$ evaporation product ^{63}Zn ; accordingly, we place only a 5-nsec upper limit on any delayed γ rays associated with these transitions.

V. DISCUSSION

The relevant single-particle shell-model orbits in this mass region are $2p_{3/2}$, $1f_{5/2}$, $2p_{1/2}$, and $1g_{9/2}$. In the neighboring odd isotope ^{65}Ga several states have been identified from transfer reactions as having large single-particle parentage.³² These are a $2p_{3/2}$ ground state, $1f_{5/2}$ first excited state at 190.6 keV, and a $1g_{9/2}$ $\frac{9}{2}^+$ state at 2037.1 keV. The corresponding states in ^{63}Ga in the level scheme of Fig. 8 are the $J^\pi = \frac{3}{2}^-$ ground state, the first excited state at $E_x = 75.4$ keV with $J^\pi = \frac{5}{2}^-$, and the $J^\pi = \frac{9}{2}^+$ level at $E_x = 2046.7$ keV. Figure 13 traces the systematic trend of the single-particle states in the odd Ga isotopes. The excitation energy of the $J^\pi = \frac{5}{2}^-$, and the $J^\pi = \frac{1}{2}^-$ states are seen to decrease gradually with decreasing neutron number, whereas the excitation energy of the $J^\pi = \frac{9}{2}^+$ states remains almost constant. (We note that the latest $A = 65$ compilation¹³ tentatively suggests $J^\pi = \frac{3}{2}^-$ for the $E_x = 62$ keV state in ^{65}Ga . In the absence of a rigorous assignment, we assume $J^\pi = \frac{1}{2}^-$ for this state in the subsequent discussion; the latter assignment has been suggested several times in the literature.^{33,34}) No $J^\pi = \frac{1}{2}^-$ level was identified in ^{63}Ga , most likely due to the fact that the reaction mechanism used selectively populates yrast states. Heavy-ion fusion evaporation reaction studies of the neighboring odd isotopes ^{65}Ga and ^{67}Ga did not observe the respective $J^\pi = \frac{1}{2}^-$ single-particle states in these nuclei previously established in light-ion work.^{9,11} As noted above, the present work suggests that the $B(E2)$ for the $(\frac{5}{2}^-)_1 \rightarrow (\frac{3}{2}^-)_1$ transition in ^{63}Ga shows some collective character, in contrast to the heavier odd Ga isotopes. Unfortunately, because ^{62}Zn is not stable it is not possible to obtain the corresponding single-particle transfer data to investigate whether there is a corresponding discontinuity in the single-particle parentage of the $\frac{5}{2}^-$ states; for the heavier Ga isotopes, these spectroscopic factors are nearly constant as a function of N .

The excitation energy of the lowest $\frac{9}{2}^-$ level in the odd Ga isotopes is observed to decrease with N , following the $\frac{5}{2}^-$ states rather closely. As shown in Fig. 14, the $\frac{9}{2}^-$ to $\frac{5}{2}^-$ transition energies are on average 118 ± 14 keV higher

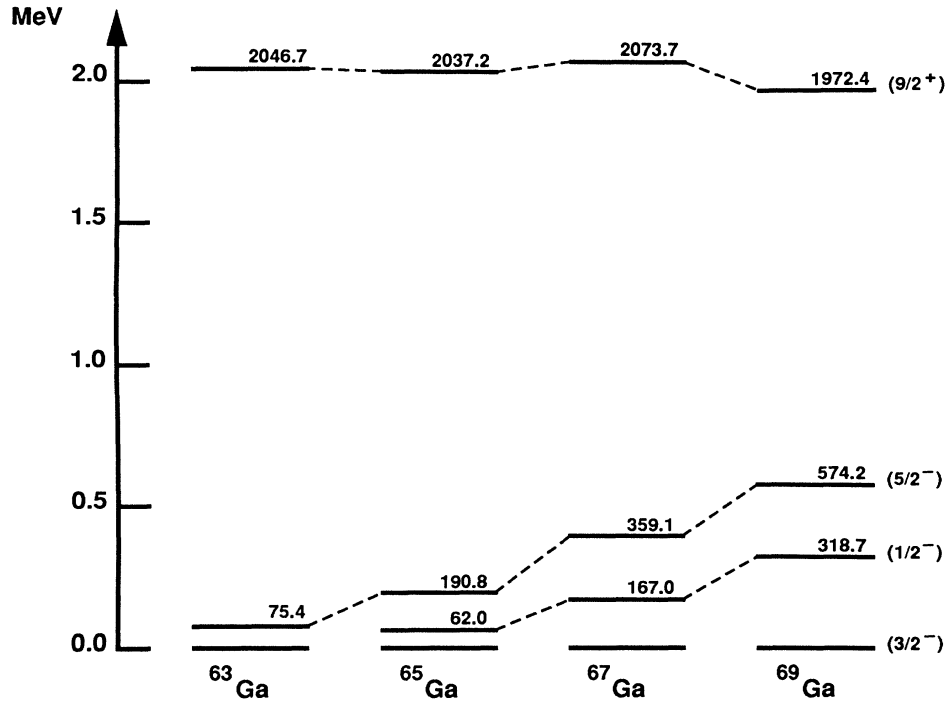


FIG. 13. Systematics of the low-lying single particle states of the neutron-deficient odd Ga isotopes.

than the 2^+ to 0^+ g.s. transitions of the corresponding even-even Zn cores and show an almost identical gradual decrease in energy with decreasing neutron number. This suggests a possible interpretation of the $\frac{9}{2}^-$ states as an $f_{5/2}$ quasiparticle coupled to the first excited 2^+ of the neighboring core. A similar interpretation has been suggested by Kawakami *et al.* for the $\frac{9}{2}^-$ state in ^{65}Ga .¹¹ In such a weak-coupling picture the $\frac{9}{2}^-$ states have unique parentage, whereas the other negative parity states in the multiplet can mix with states in the multiplets formed by coupling either a $p_{3/2}$ or a $p_{1/2}$ proton to the same core.

Most of the states so formed would be nonyrast, and therefore difficult to observe in experiments such as those of the present study. (Many low-spin negative parity states are in fact known in the less neutron-deficient Ga isotopes.) The weak coupling picture does not seem to give any useful guidance concerning either the spin or the placement of the intermediate state in the side branch from the $\frac{9}{2}^-$ state to the g.s.

The systematics of the positive parity levels in the neutron-deficient odd Ga isotopes compared to their corresponding even-even Zn cores is displayed in Fig. 15.

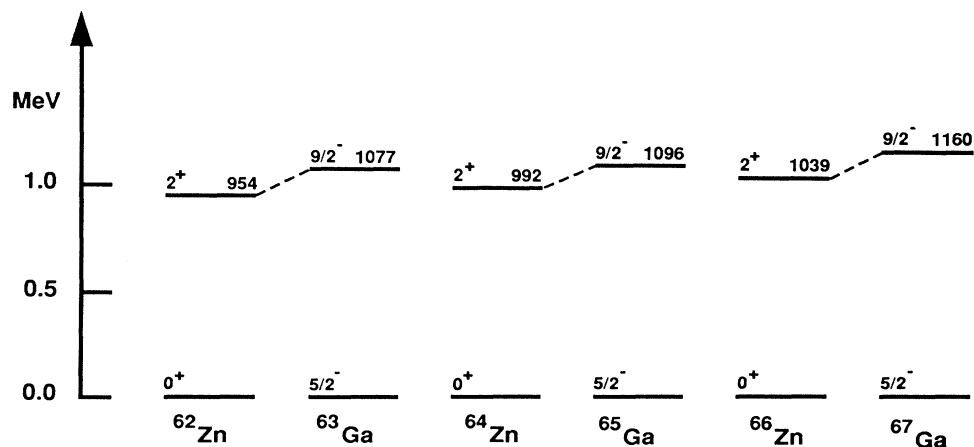


FIG. 14. Comparison of the excitation energy of the lowest $\frac{9}{2}^-$ levels in the neutron-deficient odd Ga isotopes relative to the lowest $\frac{5}{2}^-$ state with the excitation energy of the lowest 2^+ state of the corresponding Zn core.

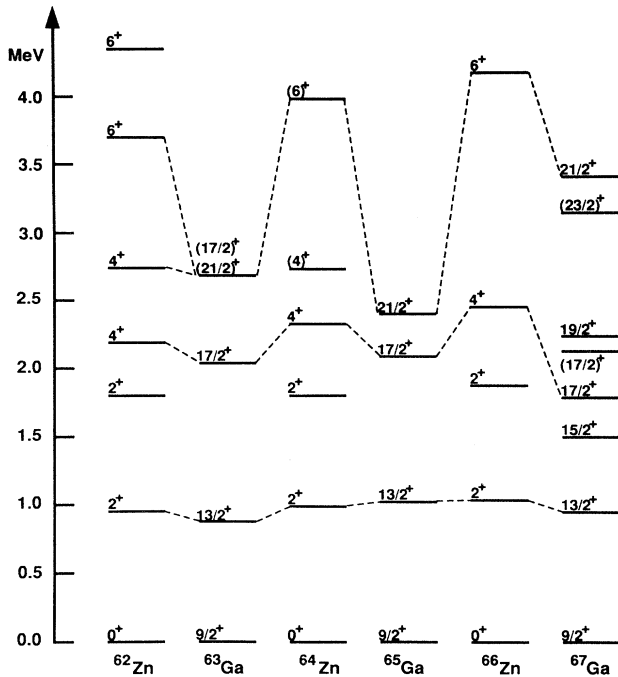


FIG. 15. Systematics of the states built on the $\pi g_{9/2}$ configuration of the neutron-deficient Ga isotopes compared to the corresponding even-even Zn cores. Excitation energies for the odd- A systems are given with respect to the energies of their respective $J^\pi = \frac{9}{2}^+$ levels.

The level energies for ^{62}Zn were obtained from Refs. 35 and 36. For the purpose of comparison the excitation energies of levels in the odd systems are shown relative to the excitation energy of the respective $J^\pi = \frac{9}{2}^+$ states. The energies of the $J^\pi = \frac{13}{2}^+$ to $J^\pi = \frac{9}{2}^+$ transitions track very closely the excitation energies of the $J^\pi = 2^+$ states of the cores and suggest an interpretation in the framework of the weak coupling model. The excitation energies of the $J^\pi = \frac{17}{2}^+$ states (with respect to the $J^\pi = \frac{9}{2}^+$ state) compared to the $J^\pi = 4^+$ states in the respective cores show much larger discrepancies depending on neutron number, increasing from 152 keV in ^{63}Ga to 222 keV in ^{65}Ga and 668 keV in ^{67}Ga . In this interpretation of the $J^\pi = \frac{17}{2}^+$ states as a $\pi g_{9/2}$ quasiparticle coupled to the

$J^\pi = 4^+$ core, the strength of the coupling would appear to decrease with decreasing neutron number.

The angular distribution of the 649.1-keV transition is consistent with $\Delta J = 0, 2$, suggesting $J^\pi = \frac{17}{2}^+$ and $J^\pi = \frac{21}{2}^+$ as possible spin assignments for its initial state. The energy difference between the initial state of the 649.1-keV transition and the second excited $J^\pi = 4^+$ state in ^{62}Zn is only 60 keV. A $J^\pi = \frac{17}{2}^+$ assignment to the 4729.3-keV state could thus be interpreted as the coupling of the $\pi g_{9/2}$ quasiparticle to the second excited $J^\pi = 4^+$ in ^{62}Zn . An argument against this interpretation is the expectation that fusion-evaporation reactions will feed yrast states. Note, however, that the 4_2^+ state in ^{62}Zn was observed under experimental conditions very similar to those of the present work.^{35,36} On the other hand, if the $J^\pi = \frac{21}{2}^+$ assignment¹¹ in ^{65}Ga is correct, the systematics would suggest $J^\pi = \frac{21}{2}^+$ for this state. We note in passing that the data in Ref. 11 for the corresponding state in ^{65}Ga appear to be consistent with a spin assignment of $\frac{17}{2}^+$ as well as the $\frac{21}{2}^+$ assignment given there. When the excitation energy of the $\frac{9}{2}^+$ state is normalized to the ground state of the ^{62}Zn core, the level schemes for ^{62}Zn and ^{63}Ga display a striking similarity, as shown in Fig. 15.

In conclusion, we have been able to identify the first in-beam transitions in ^{63}Ga and construct a level scheme with tentative spin and parity assignments. The yrast states fit rather well within the systematics of the neighboring isotopes and a comparison to excitations of the core suggests a qualitative interpretation in the framework of the weak coupling model. Finally, it should be noted that we have not been able to identify any states that could be associated with octupole degrees of freedom regarding the predictions for the ^{64}Ge core (cf. Ref. 1).

ACKNOWLEDGMENTS

The assistance of Dr. P. H. Kutt with the data acquisition and analysis is acknowledged with thanks. The targets for this work were fabricated by Laszlo Csihas. Financial support for this work was provided by the National Science Foundation. In addition, the support of the University of Pennsylvania Research Foundation in connection with the neutron detector array is acknowledged with thanks.

*Present address: Bell Communications Research, Morristown, NJ 07960.

¹J. Görres, T. Chapuran, D. P. Balamuth, and J. W. Arrison, Phys. Rev. Lett. **58**, 662 (1987).

²W. Nazarewicz *et al.*, Nucl. Phys. **A429**, 269 (1984).

³J. W. Arrison, T. Chapuran, U. J. Hüttmeier, and D. P. Balamuth, Phys. Lett. B **248**, 39 (1990).

⁴J. Heese *et al.*, Phys. Rev. C **41**, 1553 (1990).

⁵L. Lühmann, M. Debray, K. P. Lieb, W. Nazarewicz, B. Wörmann, J. Eberth, and T. Heck, Phys. Rev. C **31**, 828 (1985).

⁶J. W. Arrison, D. P. Balamuth, T. Chapuran, D. G. Popescu, J.

Görres, and U. J. Hüttmeier, Phys. Rev. C **40**, 2010 (1989).

⁷M. Wiosna, J. Busch, J. Eberth, M. Liebchen, T. Mylaeus, N. Schmal, R. Sefzig, S. Skoda, and W. Teichert, Phys. Lett. B **200**, 255 (1988).

⁸J. N. Mo and S. Sen, Nucl. Data Sheets **39**, 741 (1983).

⁹F. Kearns and N. J. Ward, Nucl. Data Sheets **35**, 101 (1982).

¹⁰M. R. Bhat and D. E. Alburger, Nucl. Data Sheets **53**, 1 (1988).

¹¹H. Kawakami, A. P. de Lima, R. M. Ronningen, A. V. Ramayya, J. H. Hamilton, R. L. Robinson, H. J. Kim, and L. K. Peker, Phys. Rev. C **21**, 1311 (1980).

¹²H. J. Rose and D. M. Brink, Revs. Mod. Phys. **39**, 306 (1967).

- ¹³N. J. Ward and J. Tuli, Nucl. Data Sheets **47**, 135 (1986).
- ¹⁴B. A. Nemashkalo, V. E. Storizhko, V. F. Boldyshev, O.I. Ekhichev, A. P. Klyucharev, and A. I. Popov, Yad. Fiz. **17**, 229 (1973) [Sov. J. Nucl. Phys. **17**, 117 (1973)].
- ¹⁵G. H. Dulfer, H. E. Beertema, and H. Verheul, Nucl. Phys. **A149**, 518 (1970).
- ¹⁶U. J. Huttmeier, D. P. Balamuth, T. Chapuran, J. W. Arrison, and D. G. Popescu, Bull. Am. Phys. Soc. **33**, 1574 (1988).
- ¹⁷T. Chapuran, D. P. Balamuth, J. W. Arrison and J. Goerres, Nucl. Instrum. Methods. A **272**, 767 (1988).
- ¹⁸P. H. Kutt and D. P. Balamuth, Comput. Phys. **3** (5), 52 (1989).
- ¹⁹C. Pastor, F. Benrachi, B. Chambon, D. Drain, A. Danchi, A. Giorni, and C. Morand, Nucl. Instrum. Methods **212**, 209 (1983).
- ²⁰R. Middleton, Nucl. Instrum. Methods **214**, 139 (1983).
- ²¹F. Pühlhofer, Nucl. Phys. **A280**, 267 (1977).
- ²²Bicron, Inc.
- ²³P. H. Kutt (unpublished).
- ²⁴D. P. Balamuth, T. Chapuran, and J. W. Arrison, Nucl. Instrum. Methods A **275**, 315 (1989).
- ²⁵K. Alder, A. Bohr, T. Huus, B. Mottelson, and A. Winther, Revs. Mod. Phys. **28**, 432 (1956).
- ²⁶L. Cleemann, J. Eberth, W. Neumann, N. Wiehl, and V. Zobel, Nucl. Phys. **A334**, 157 (1980).
- ²⁷C. Morand *et al.*, Nucl. Phys. **A308**, 103 (1978).
- ²⁸N. Schmal *et al.*, in *Proceedings of the International Symposium on In-Beam Nuclear Spectroscopy, Debrecen, Hungary, 1984*, edited by Zs. Dombardi and T. Fenyés (Akademiai Kiado, Budapest, Hungary, 1985).
- ²⁹L. Hildingsson, C. W. Beausang, D. B. Fossan, W. F. Piel, Jr., A. P. Byrne, and G. D. Dracoulis, Nucl. Instrum. Methods **252**, 91 (1986).
- ³⁰M. Nurmia, R. W. Fink, Phys. Lett. **14**, 136 (1965).
- ³¹R. L. Auble, Nucl. Data Sheets **14**, 1 (1975).
- ³²B. Zeidman, R. H. Siemssen, G. C. Morrison, and L. L. Lee, Jr., Phys. Rev. C **9**, 409 (1974).
- ³³M. G. Betigeri, H. H. Duhm, R. Santo, R. Stock, and R. Bock, Nucl. Phys. **A100**, 416 (1967).
- ³⁴R. G. Couch, J. A. Biggerstaff, F. G. Perey, and S. Raman, Phys. Rev. C **2**, 149 (1970).
- ³⁵L. Mulligan, R. W. Zurmühle, and D. P. Balamuth, Phys. Rev. C **19**, 1295 (1979).
- ³⁶N. J. Ward, L. P. Ekström, G. D. Jones, F. Kearns, T. P. Morrison, O. M. Mustafa, D. N. Simister, P. J. Twin, and R. Wadsworth, J. Phys. G **7**, 815 (1981).